Journal of
Applied Remote Sensing

Statistical estimation of a 13.3 μm Visible Infrared Imaging Radiometer Suite channel using multisensor data fusion

James Cross
Irina Gladkova
W. Paul Menzel
Andrew Heidinger
Michael D. Grossberg

SPIE

Statistical estimation of a 13.3 μm Visible Infrared Imaging Radiometer Suite channel using multisensor data fusion

James Cross,[a] Irina Gladkova,[a] W. Paul Menzel,[b] Andrew Heidinger,[c] and Michael D. Grossberg[a]

[a]City College of New York, Department of Computer Science, 160 Convent Avenue, New York, New York 10031
james.henry.cross.iii@gmail.com
[b]CIMSS/University of Wisconsin, 1225 West Dayton Street, Madison, Wisconsin 53706
[c]NOAA/NESDIS/STAR, 1225 West Dayton Street, Madison, Wisconsin 53706

Abstract. We describe an algorithm for creating a virtual, statistically estimated 13.3-μm band for the Visible Infrared Imaging Radiometer Suite (VIIRS), an instrument aboard the National Oceanic and Atmospheric Administration's (NOAA's) operational satellite, Suomi NPP. VIIRS does not have a 13.3-μm band, although this band has important applications such as estimating cloud-top pressure. We demonstrate that a reliable estimate of the missing data can be created with a multisensor approach, using other VIIRS bands at 4, 9, 11, and 12 μm, as well as input from the Cross-track Infrared Sounder, on board the same satellite, which produces data at a much finer spectral resolution but lower spatial resolution. In addition, we evaluate the algorithm by applying it to data from the Moderate Resolution Image Spectroradiometer (MODIS) and the Atmospheric Infrared Sounder (AIRS), both on the Aqua satellite. MODIS and AIRS provide a benchmark for measuring the accuracy of the algorithm since, unlike VIIRS, MODIS makes measurements in the 13.3-μm band. [DOI: 10.1117/1.JRS.7.073473]

Keywords: data fusion; statistical estimation; Visible Infrared Imaging Radiometer Suite; multisensor.

Paper 13284 received Aug. 2, 2013; revised manuscript received Oct. 28, 2013; accepted for publication Oct. 30, 2013; published online Nov. 27, 2013.

1 Introduction

Meteorologists and other scientists rely heavily on data collected from instruments aboard orbiting satellites, for example, to create accurate estimates of physical parameters with important applications, such as cloud-top pressure (CTP). The design of such instruments, however, requires technical and economic trade-offs that often result in certain desirable data not being directly available. One way to mitigate this deficiency is to use machine learning techniques to estimate the values that are not directly observed. This can be accomplished by exploiting statistical correlation with information in available data sets. By combining the information from multiple sources, it is often possible to create an accurate estimate of the physical quantities that are not directly available.[1]

Cloud properties provide a good example of scientifically important physical attributes, which can be determined using information from satellite instruments. Clouds are an important subject in climate studies because of their dominant role in Earth's energy balance and water cycle. Cloud visible reflectivity and infrared trapping have significant impact on weather systems and climate changes.[2] Historically, the sensor used to make such important products has evolved or changed as satellite missions have been completed. This introduces challenges in maintaining the consistency of long-term descriptions of cloud trends in the face of sensor changes from Polar-Orbiting Environmental Satellite to Earth Observing System (EOS) to Joint Polar

0091-3286/2013/$25.00

Satellite System (JPSS) platforms. With the October 2011 launch of the Suomi National Polar Partnership (SNPP), the Visible and Infrared Imaging Radiometer Suite (VIIRS) became the operational imager for the afternoon National Oceanic and Atmospheric Administration (NOAA) environmental polar orbiting satellite.[3] Additionally, the Cross-track Infrared Sounder (CrIS), which is a Fourier transform spectrometer, became the operational sounder.

However, VIIRS does not have any infrared spectral bands located in H_2O or CO_2 absorption bands, which degrades its ability to determine semitransparent cloud properties (including CTPs/heights) compared to that of sensors including even a single absorption channel.[4] In an effort to ensure continuity and consistency between historical cloud products and those provided from the SNPP sensors (and JPSS in the future), we demonstrate a VIIRS plus CrIS cloud algorithm that can extend the cloud record created using data from the Advanced Very High Resolution Radiometer (AVHRR) and the High Resolution Infrared Radiation Sounder (HIRS), as well as from the Moderate Resolution Image Spectroradiometer (MODIS) and the Atmospheric Infrared Sounder (AIRS). VIIRS has 16 spectral bands measured at 750-m resolution at nadir, all making the measurements in the visible and infrared spectrum. This article presents a technique to generate an additional VIIRS channel at 13.3 μm statistically constructed from CrIS and VIIRS measurements. The CrIS sensor makes 1305 high spectral resolution measurements at ~15-km resolution. These narrow bandwidth CrIS measurements are convolved with a spectral response function for the desired 13.3-μm band at the lower 15-km CrIS resolution. These values are then used in conjunction with other infrared spectral bands on VIIRS at 750-m resolution to create a virtual 13.3 μm channel at 750-m resolution using statistical estimation. The observed VIIRS channels combined with the statistically constructed 13.3 μm channel are then used in a CTP algorithm that has been developed for the pending Advanced Baseline Imager (ABI) to be launched in 2015 on the Geostationary Operational Environmental Satellite-R Series (GOES-R).[5]

Estimation of VIIRS 13.3-μm band fits into a broadly defined image fusion framework as defined in Ref. 1. A large collection of fusion algorithms use a framework known as "pan-sharpening." These methods work with multispectral images of different resolutions to produce one or more high resolution images combining information from different channels. A look-up table approach has also been successfully used to estimate one band using other bands from the same source.[6] However, both the methodology and goal of this work differ from these approaches. Although these methods aim to produce a visualization which combines features from different sources, our goal is quite different. In our case, the synthetic 13.3-μm band is intended to be used in algorithms to create data products, such as the CTP product described below, in place of a measured band which is not available. Thus, the assessment of the quality of a synthetic band is the accuracy of derived products using the estimated data.

In developing and evaluating our algorithm, we used data from MODIS, an instrument aboard the NASA satellites Aqua and Terra, which is a part of EOS.[7] MODIS and VIIRS share some of the same bands. In particular, MODIS bands 23, 29, 31, and 32 (4, 8.5, 11, and 12 μm) have characteristics similar to the M13, M14, M15, and M16 bands of VIIRS. Furthermore, MODIS band 33 is centered at 13.3 μm, which is the target spectral band, and has all of the resolution, location, and temporal characteristics desired. Just as the Suomi NPP satellite carries both VIIRS and CrIS, the Aqua satellite carries MODIS and the infrared sounder AIRS. Like CrIS, AIRS covers the target spectral response range around 13.3 μm (through a multitude of narrow bands), and like CrIS at a much lower spatial resolution.[8] For both pairs (VIIRS/CrIS and MODIS/AIRS), the two instruments on the same satellite share largely overlapping observation areas, though in each case, the high spectral resolution sounder has less cross-track coverage than the high spatial resolution imager (see Fig. 1). Hence, for our evaluation, we treat the directly observed 13.3-μm band on MODIS as our truth and test our 13.3 μm estimation algorithm by applying the algorithm to MODIS/AIRS bands corresponding to the same bands on VIIRS/CrIS. The results of these tests are described in Sec. 3.

It is assumed in this work that there exists an unknown function from bands available on VIIRS to the target 13.3-μm band, at least locally. We will show that this assumption holds by testing it with a representative set of MODIS and AIRS granules as a proxy for VIIRS and CrIS. In addition, to compute the function which produces 13.3 μm estimated values, we will assume a measure of scale invariance in the relationship between available source bands and the desired

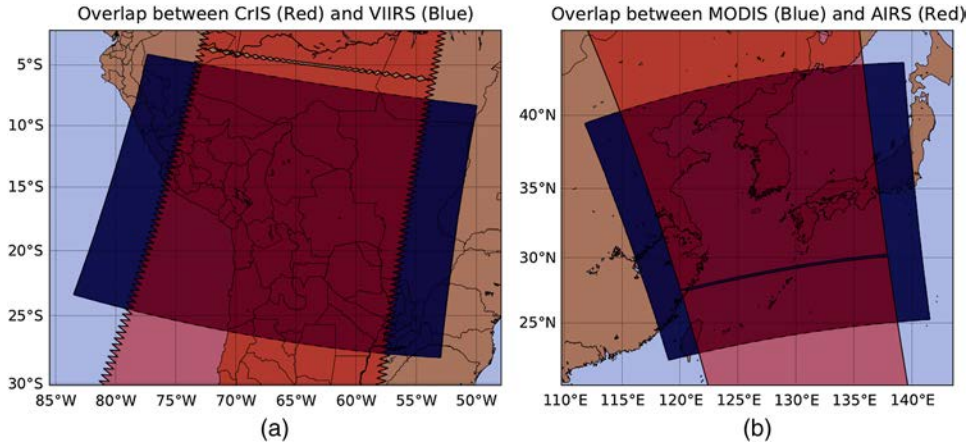

Fig. 1 Mapped image showing overlap between VIIRS granule over South America (September 19, 2012) and corresponding CrIS (a); overlap between MODIS granule over the Korean Peninsula (May 23, 2004) and corresponding AIRS (b).

band. This assumption makes it possible to establish a relationship between a vector of radiance values in the source bands and the scalar radiance value in the desired band for low resolution images and to apply the same relationship to high resolution images. We will provide evidence for the validity of this assumption. It should be noted that this algorithm does not rely on attributes specific to the 13.3-μm band, and thus this approach might be applicable to other instances where data from a particular spectral band is not available at the high spatial resolution, though this is beyond the scope of this article.

The remainder of this article is organized as follows. Section 2 describes the estimation algorithm in detail. Section 3 validates the algorithm by applying it to representative sets of overlapping MODIS and AIRS granules where there is known truth and describes the results of using the virtual 13.3-μm band in the generation of CTP, a data product with important meteorological applications. Section 4 presents the results when the multisensor fusion approach is applied to VIIRS and CrIS granules, also showing a strong qualitative correlation with nearly coincident MODIS results.

2 Statistical Estimation

In this section, we will briefly describe our method for the statistical estimation of the 13.3-μm band. We note that the algorithm is not specific to estimating this particular spectral band. Rather it relies on having available bands at the same (relatively high) spatial resolution as the desired band as well as lower resolution measurements covering the spectral range of the desired band. This lower resolution band, in our case, will in turn be estimated from a set of images from a hyperspectral sounder whose spectral sampling range includes the broad band response of the target 13.3-μm band.

A block diagram of the estimation algorithm is shown in Fig. 2. (In this article, a tilde indicates that values are computed rather than measured, superscripts indicate spatial resolution, and subscripts indicate central wavelength.). The top right of the diagram shows how the target 13.3-μm band is built at this same lower spatial resolution using the known 13.3 μm spectral response function (see Fig. 3: in this work, we have used the spectral response function for band 33 of MODIS). The left side of the figure shows how the high-resolution (VIIRS) input bands are spatially downsampled to the resolution of the hyperspectral sounder (CrIS) using geographic information from both instruments (see Fig. 4). These two data sets, now at the same spatial resolution (designated $\tilde{R}_{\nu}^{L}$ and $\tilde{R}_{\lambda}^{L}$ for the input and target bands, respectively), are then used to build a function, designated F, mapping the input bands which are known for VIIRS to the desired 13.3-μm band at a lower resolution:

$$\tilde{R}_{\lambda}^{L} = F(\tilde{R}_{\nu}^{L}).$$

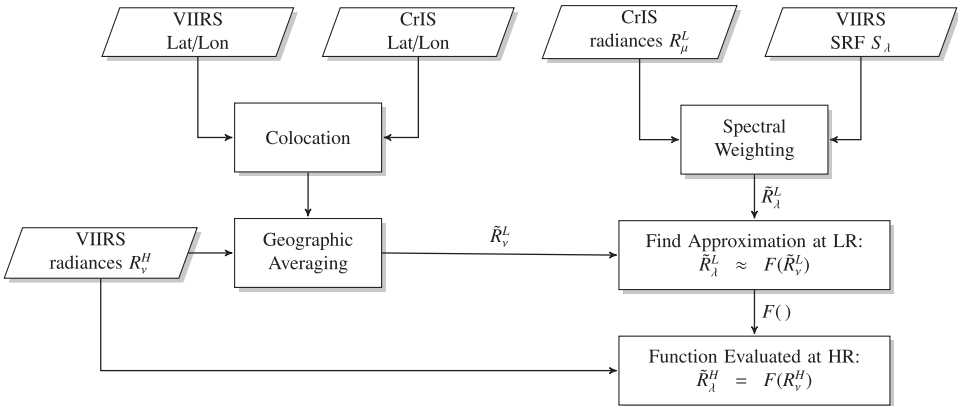

Fig. 2 Block diagram of statistical estimation algorithm.

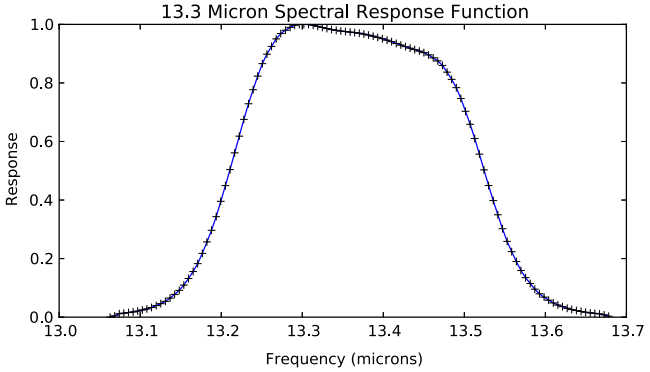

Fig. 3 The "+" markers indicate the spectral response values at 109 central wavelengths where AIRS measurements are available.

This function is then applied to the high-resolution VIIRS measurements to estimate the missing 13.3-μm band for VIIRS, represented by

$$\tilde{R}_\lambda^H = F(R_\nu^H).$$

It should be noted that for the estimating function F to provide a meaningful approximation, it should be the case that the local variance of the 13.3 μm values should be small in a neighborhood of a fixed value for the input bands, implying an essentially smooth function. To demonstrate that this property indeed holds, we use MODIS data since it measures 13.3 μm as well as the input bands. Visualizing the relationship as a scatter plot would require one output and four inputs, or a total of five dimensions. To create a three-dimensional visualization we have taken the x-y plane to be projections into the first 2 principal component analysis (PCA) components of the input variables, for Fig. 5, with the z-axis being the corresponding value in the 13.3-μm band. It is clear from the figure that, indeed, the relationship of the input bands to the target band is essentially a function. It should also be noted that for the estimation algorithm to work, the function F must be invariant across different spatial resolutions. The consistency of least-square coefficients describing this relationship at various spatial resolutions, which can be seen in Fig. 6, illustrates that this is the case.

In practice, the estimation performs best when the estimating function F is a piecewise approximation which varies with geographic location. Thus, we extend F so that it takes the longitude and latitude as input arguments in addition to requiring the source radiance values. To estimate the target radiance at a given pixel, the vector of radiance values for the source bands at high resolution and its corresponding geographic coordinates are used to query the database.

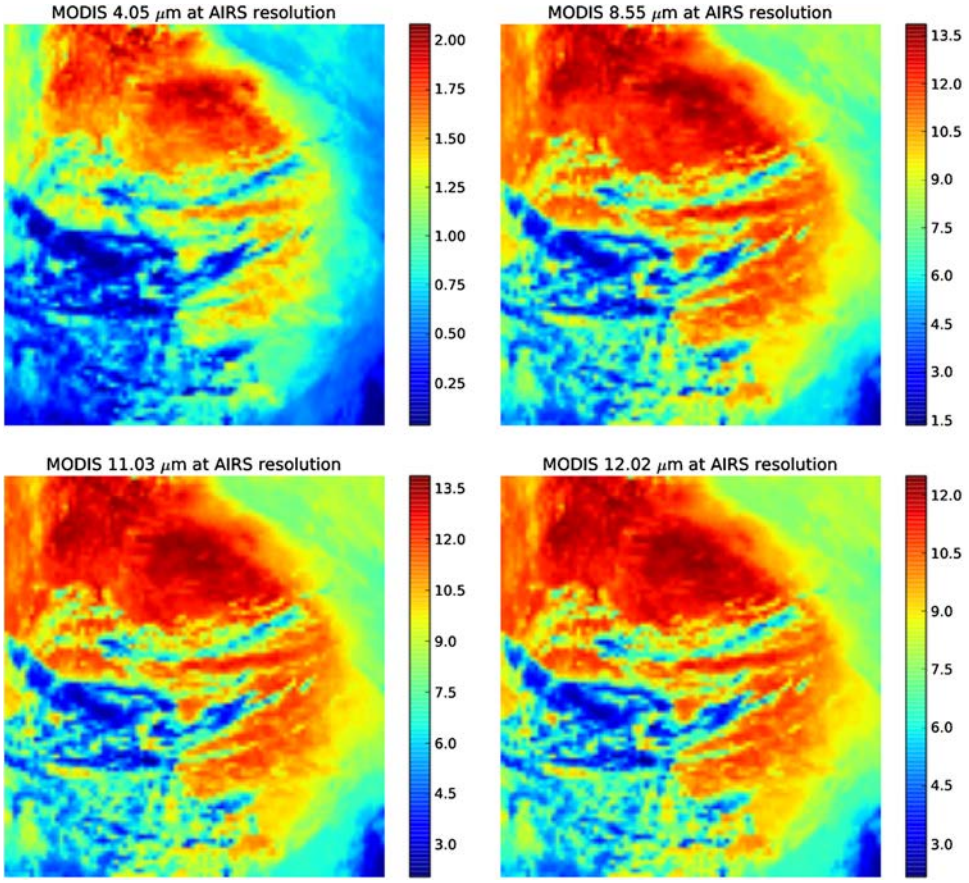

Fig. 4 Lower spatial resolution radiance values $\tilde{R}_{\nu}^{L}$ computed from the known bands. The original available bands of MODIS were degraded to AIRS resolution using geographic collocation data and used in the estimation block of the diagram as independent variables.

The query is efficiently executed using the k-d tree data search algorithm[9] to find k-nearest neighbors.[10] For this article, the scale factor combining radiance and coordinates into distance, as well as $k = 5$, was determined empirically. For each input pixel, the query finds the five pixels among the low-resolution training data set, which are closest to the input values in the six-dimensional space representing the four input bands and two additional geographic dimensions.

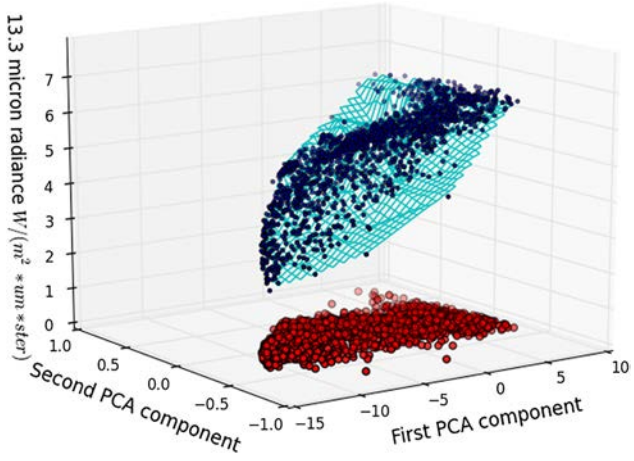

Fig. 5 Scatter plot of the target 13.3-μm band radiance values (from MODIS) (z-axis) as a function of the four input bands radiances projected into two PCA components (x-y plane) for visualization. The fact that the points occur on or near the surface is evidence that the target band can be well estimated as a function of the input bands.

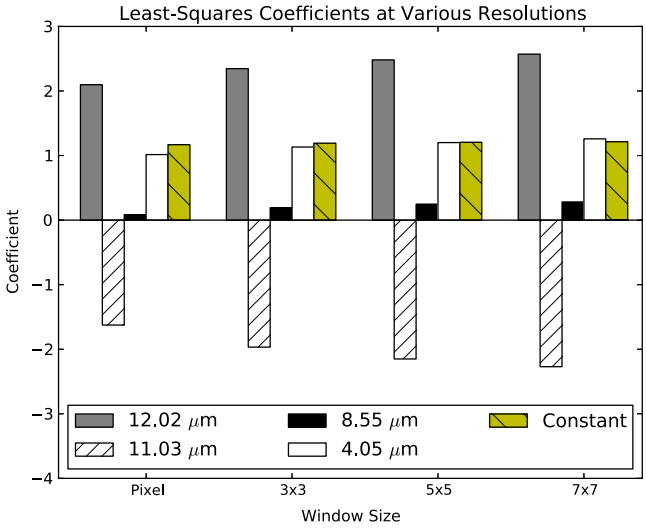

Fig. 6 Least-square coefficients describing the relationship between four MODIS bands (known on VIIRS) to the 13.3-μm band at various spatial resolutions.

The corresponding 13.3 μm values for these neighbors are then averaged to create an estimated value for each pixel at the higher resolution in the target 13.3-μm band.

3 Fusion Results on MODIS/AIRS

To evaluate our algorithm, we require truth values R_λ^H since the error of our estimates is given by the mean square errors $|R_\lambda^H - \tilde{R}_\lambda^H|^2$. Since the 13.3 μm values are unavailable for VIIRS, we use MODIS images as a proxy for VIIRS and AIRS hyperspectral data as a proxy for CrIS hyperspectral data. In this section, we describe our testing of seven instances in which a MODIS/AIRS pair is used as proxy for VIIRS/CrIS, which demonstrates consistent results across a variety of granules, with the statistical estimation of a 13.3-μm channel at MODIS resolution providing a very close estimate of the actual MODIS 13.3-μm channel.

The normalized RMSE figures between the estimated and actual 13.3 μm data for each of the seven test cases, for both all pixels and overlap pixels only, can be seen in Fig. 7. The consistent performance of the algorithm can be seen in Fig. 8, which shows envelopes for the relative error distributions among all seven test instances, one with all pixels included

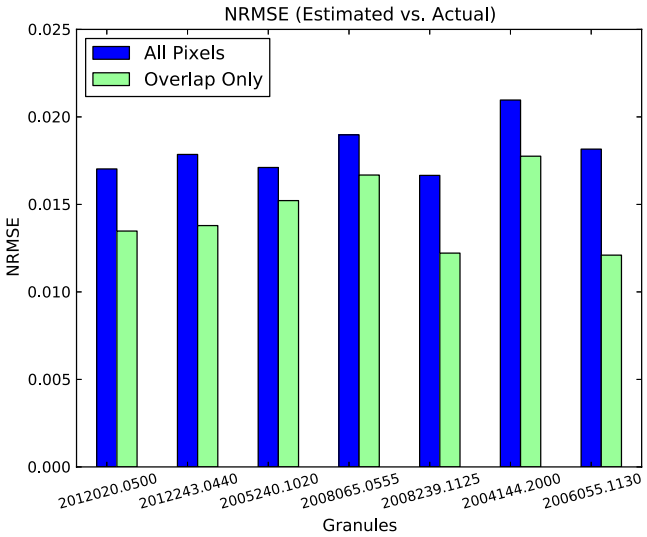

Fig. 7 Errors between the estimated 13.3-μm channel and the actual MODIS 13.3-μm channel for seven test cases.

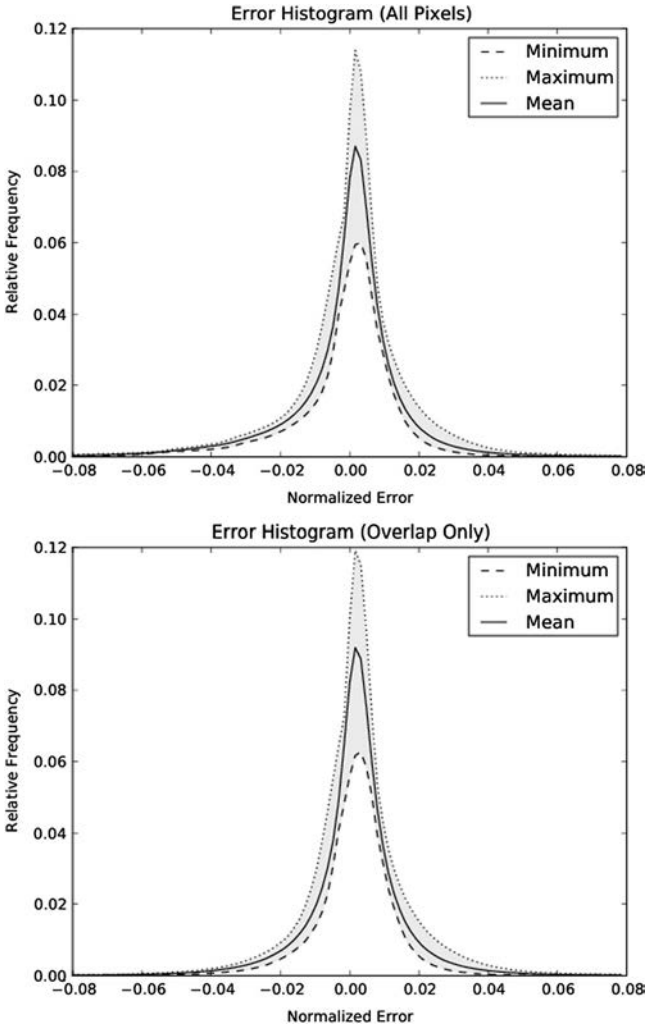

Fig. 8 Histogram of errors among all pixels for MODIS/AIRS 13.3 μm estimation.

and the other considering only pixels where MODIS and AIRS overlap. The average error distribution for each case is also shown.

In addition to testing the 13.3 μm values produced by our estimation against the known MODIS 13.3-μm band, we tested it as input values to an algorithm which estimates CTP using data from 11-, 12-, and 13.3-μm bands. This algorithm was developed for the GOES-R satellite, planned for launch in late 2015 carrying the ABI instrument, which will measure 13.3-μm band (at 2-km spatial resolution).[11] One example of such CTP values created with

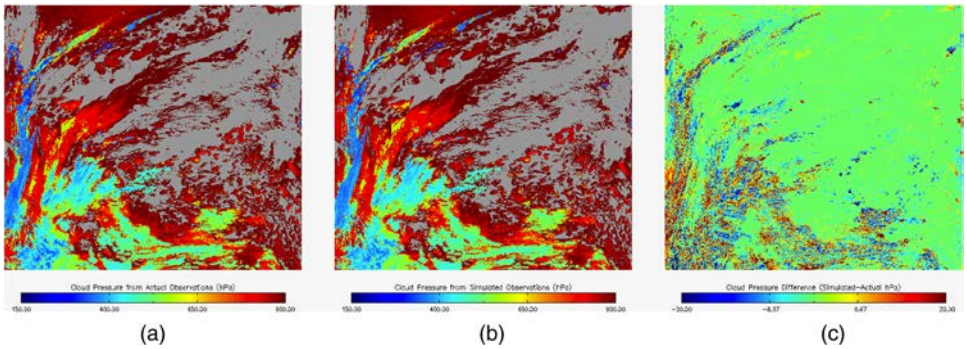

Fig. 9 Cloud-top pressure (CTP) product: original 13.3-μm band (a) and estimated (b), and difference (c). Case 1: MODIS Aqua granule MYD021KM.A2012020.0500.

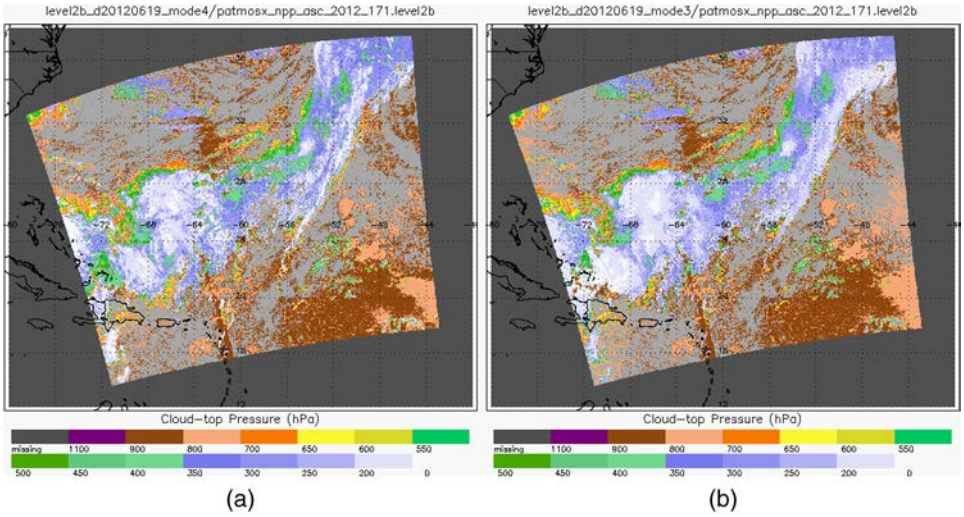

Fig. 10 June 19, 2012, CTPs with no 13.3 μm data derived with VIIRS algorithm (a) and from the ABI algorithm using VIIRS measurements and the statistically reconstructed 13.3-μm channel (b).

actual and synthesized 13.3 μm data, as well as their difference, can be seen in Fig. 9. These tests showed that similarly synthesized data from VIIRS and CrIS would allow VIIRS/CrIS to match GOES-R in terms of CTP determination, to within the GOES-R specifications. This is especially important for getting such values for night scenes since VIIRS relies on data in the visible to near-infrared range during the day, but must complement infrared window data at night with the the synthesized 13.3 μm data.

4 Fusion Results on VIIRS/CrIS

In this section, we pursue the statistical estimation of a 13.3-μm channel for VIIRS data using the collocated CrIS measurements. As in the previous section, we convolve the CrIS high spectral resolution measurements with the MODIS channel 33 spectral response function to create broadband 13.3 μm measurements at the CrIS resolution. Then, a regression relationship is made between those measurements and spatially collocated VIIRS M13, M14, M15, and M16 measurements aggregated to the CrIS spatial resolution. Thereafter, that regression relationship is applied to full resolution VIIRS 750 m measurements to achieve statistically estimated VIIRS 13.3 μm spectral band measurements.

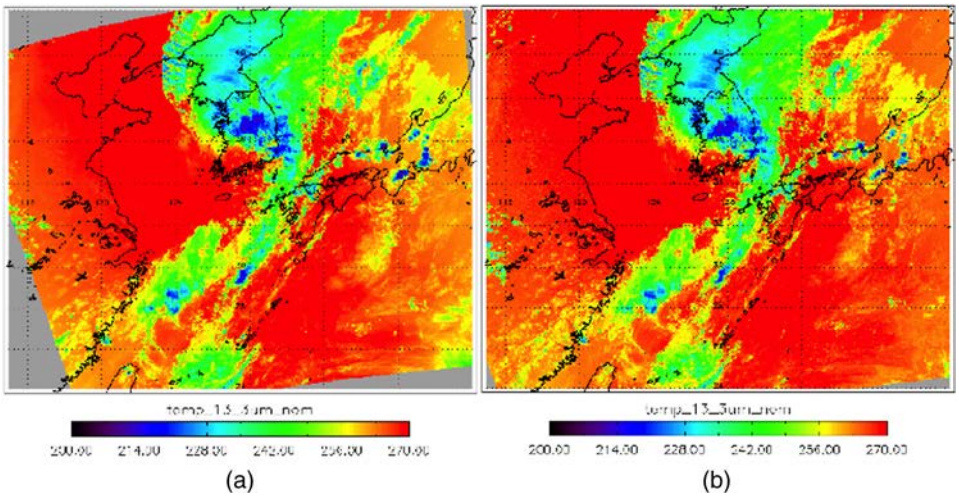

Fig. 11 August 28, 2012 MODIS measured 13.3 μm brightness temperatures at 4:30 UTC (a) and VIIRS statistically reconstructed 13.3 μm brightness temperatures (b) at 4:40 UTC.

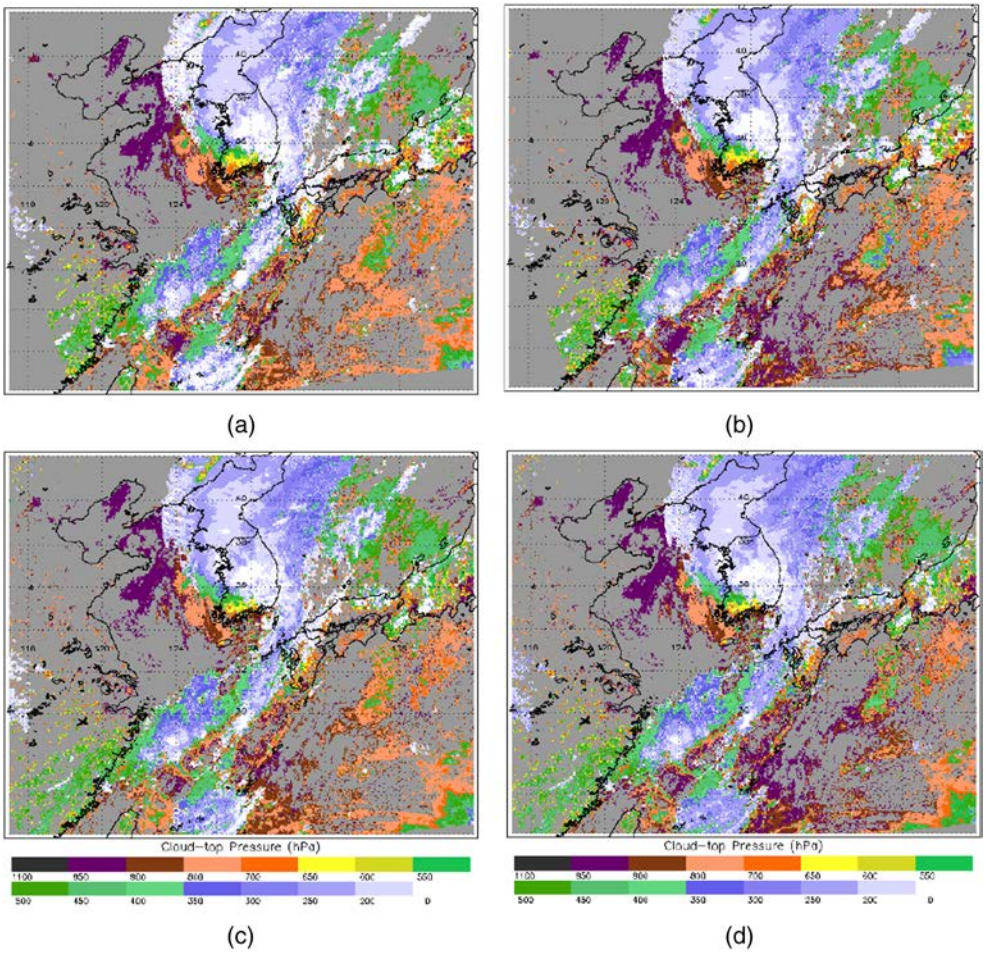

Fig. 12 August 28, 2012, MODIS measurements at 04:30 UTC and (a-b) from VIIRS measurements and the statistically reconstructed from CrIS 13.3-μm channel at 04:40 UTC (c-d). CTPs derived using MODIS data and VIIRS algorithm (a); from MODIS data and ABI algorithm, the state of the art (b); VIIRS data and VIIRS algorithm (c); and VIIRS data (with estimated 13.3-μm band) and ABI algorithm (d).

Figure 10 shows an example of CTP generated from VIIRS data both with and without the estimated 13.3-μm band. The granule includes a significantly cloudy scene over the western Atlantic Ocean, from June 19, 2012. The values on the left are derived without the 13.3 μm data using an optimal estimation approach that relies on the NCEP Global Data Assimilation System as a first guess. The values on the right are calculated with the ABI algorithm using the statistical estimation produced with the CrIS information in addition to the existing VIIRS channels.

For another example, over the Korean peninsula on August 28, 2012, MODIS and VIIRS data are available covering the same area and separated in time by only 10 min (cf. Fig. 11). This allows us to qualitatively evaluate the difference between CTP values created from MODIS with the ABI algorithm using true 13.3 μm values (the state of the art) and those created from VIIRS using the reconstructed 13.3 μm values. Both can then be compared to the CTP values made from those data sets using the VIIRS algorithm, which requires no 13.3 μm values. On this day, deep convection over the southern part of the Korean peninsula created a cirrus outflow to the northwest; the heights of these semitransparent cirrus clouds are hard to determine without a semitransparency correction offered by the 13.3 μm data. In addition, low clouds are present over the ocean south of Japan where only infrared window techniques tend to place the cloud at the ocean surface rather than just above because there is little thermal contrast between cloud and clear sky. In high thin cirrus west of North Korea, the ABI

algorithm with the 13.3 μm data gets the CTP at 250 hPa, while the VIIRS optimal estimation without the 13.3 μm data pins it at the tropopause. In low clouds over the Pacific Ocean south of Japan, the 13.3 μm data helps the cloud algorithm move the clouds off the ocean surface, in better agreement with MODIS results. The discrepancy is very similar to that between CTPs from VIIRS using the artificial 13.3 μm band and those created using the extant VIIRS algorithm. This strongly supports the usefulness of the statistically estimated 13.3 μm VIIRS band. All four images can be seen in Fig. 12.

5 Conclusion

With examples using both Aqua MODIS and AIRS data as well as Suomi NPP VIIRS and CrIS data, we demonstrate that a reliable estimate of the imager 13.3 μm broadband radiance data can be statistically estimated from the high spectral resolution infrared sounder data and high spatial resolution imager radiances measures at 4, 8.6, 11, and 12 μm. We have successfully tested the resulting data as input values to an algorithm which estimates CTP using data from 11-, 12-, and 13.3-μm bands; we find a good agreement between VIIRS and MODIS CTPs when VIIRS has the assistance from the estimated 13.3-μm channel. These example results suggest that synergistic use of VIIRS and CrIS measurements can overcome the absence of a 13.3 μm channel on VIIRS. The central assumption required by the algorithm is that the functional relationship between the input and output bands are scale invariant (see Fig. 6). An interesting topic for future investigation is to determine other ensembles of bands where this relationship holds and thus a higher resolution spectral band may be estimated even when it is not directly measured.

References

1. L. Wald, "Some terms of reference in data fusion," *IEEE Trans. Geosci. Remote Sens.* **37**(3), 1190–1193 (1999), http://dx.doi.org/10.1109/36.763269.
2. K. E. Trenberth, J. T. Fasullo, and J. Kiehl, "Earth's global energy budget," *Bull. Am. Meteorol. Soc.* **90**(3), 311–323 (2009), http://dx.doi.org/10.1175/2008BAMS2634.1.
3. D. Hillger et al., "First-light imagery from Suomi NPP VIIRS," *Bull. Am. Meteorol. Soc.* **94**(7), 1019–1029 (2013).
4. A. K. Heidinger et al., "Using CALIPSO to explore the sensitivity to cirrus height in the infrared observations from NPOESS/VIIRS and GOES-R/ABI," *J. Geophys. Res. Atmos.* **115**(D4) (2010).
5. A. K. Heidinger, "Algorithm theoretical basis document ABI cloud height," NOAA NESDIS Center for Satellite Applications and Research, http://www.goes-r.gov/products/ATBDs/baseline/Cloud_CldHeight_v2.0_no_color.pdf (2011).
6. S. D. Miller et al., "A case for natural colour imagery from geostationary satellites, and an approximation for the GOES-R ABI," *Int. J. Remote Sens.* **33**(13), 3999–4028 (2012), http://dx.doi.org/10.1080/01431161.2011.637529.
7. I. Gladkova et al., "Statistical estimation of a 13.3 micron channel for VIIRS using multisensor data fusion with application to cloud-top pressure estimation," in *Proc. AMS 29th Conference on Environmental Information Processing Technologies*, Austin, TX (2013).
8. H. H. Aumann et al., "AIRS/AMSU/HSB on the Aqua mission: design, science objectives, data products, and processing systems," *IEEE Trans. Geosci. Remote Sens.* **41**(2), 253–264 (2003), http://dx.doi.org/10.1109/TGRS.2002.808356.
9. J. L. Bentley, "Multidimensional binary search trees used for associative searching," *Commun. ACM* **18**(9), 509–517 (1975), http://dx.doi.org/10.1145/361002.361007.
10. R. Weber, H.-J. Schek, and S. Blott, "A quantitative analysis and performance study for similarity-search methods in high-dimensional spaces," in *24th International Conf. on Very Large Data Bases*, New York, NY, Vol. 98, pp. 194–205 (1998).
11. T. J. Schmit et al., "Introducing the next-generation advanced baseline imager on GOES-R," *Bull. Am. Meteorol. Soc.* **86**(8), 1079–1096 (2005), http://dx.doi.org/10.1175/BAMS-86-8-1079.

James Cross received his BS in computer science and BA in French from Auburn University in 2002, and his JD from New York University in 2005. He is currently pursuing a PhD in computer science at the Graduate Center of the City University of New York (CUNY) with a focus on machine learning.

Irina Gladkova received the BSc degree in mathematics from Donetsk State University, Donetsk, Ukraine, in 1989, the PhD degree in physical/mathematical sciences from the Institute of Applied Mathematics and Mechanics, National Academy of Sciences of Ukraine, Donetsk, in 1993, and the PhD degree in mathematics from The Graduate Center, The City University of New York (CUNY), New York, in 1998. Since 1998, she has been a Faculty Member with The City College of New York, CUNY, where she is currently an associate professor with the Department of Computer Science. She works extensively with engineers and scientists on a variety of applied problems in the area of signal processing. Her main current interests include radar waveform design and satellite data analysis/compression.

W. Paul Menzel received his PhD in solid state physics from the University of Wisconsin in 1974. Thereafter, at the Space Science and Engineering Center (SSEC), he developed applications for Earth remote sensing using geosynchronous multispectral measurements. In 1983, he became leader of the NESDIS advanced satellite products project, responsible for transitioning research advances into operations. In 1999, as NOAA senior scientist, he participated in planning the evolution of NOAA's environmental remote sensing assets. In 2007, he rejoined UW as the Verner E. Suomi distinguished professor. Currently he is a senior scientist at SSEC where he studies global cloud trends using HIRS and MODIS measurements.

Andrew Heidinger works at the Center for Satellite Applications and Research at NOAA/NESDIS in Madison, WI. His research involves many aspects of cloud remote sensing with satellites including calibration, algorithm development, radiative transfer and climate studies. He has authored more than 80 journal papers and also serves as an adjunct faculty at the University of Wisconsin Department of Atmospheric and Oceanic Sciences.

Michael D. Grossberg received the PhD degree in mathematics from the Massachusetts Institute of Technology, Cambridge, in 1991. He was a lecturer with the Computer Science Department, Columbia University, New York, where he was also a Ritt assistant professor of mathematics. He spent four years as a research scientist with the Columbia Automated Vision Environment, Columbia University. He has authored and coauthored papers that have appeared in International Conference on Computer Vision, European Conference on Computer Vision, and Computer Vision and Pattern Recognition. He has filed several U.S. and international patents for inventions related to computer vision, as well as for multispectral image compression. He has also developed algorithms for medical imaging segmentation and satellite image compression and restoration. His research in computer vision has included topics in the geometric and photometric modeling of cameras, and analyzing features for indexing.